ZANCO Journal of Pure and Applied Sciences

TYPE Original article
DOI http://dx.doi.org/10.21271/ZJPAS.37.4.11

OPEN ACCESS

*Corresponding author

Nayla Faiq Othman

nayla.othman@epu.edu.iq

RECEIVED :06 /01 /2025
ACCEPTED :12/05/ 2025
PUBLISHED :31/ 08/ 2025

KEYWORDS:

Deep Convolutional Generative Adversarial Networks (DCGAN), Magnetic Resonance Imaging (MRI), Artificial Intelligence (AI), Deep learning (DL)

Enhancing Brain Tumor Classification Accuracy Using Deep Learning with Real and Synthetic MRI Images

Nayla Faiq Othman[1*] and Shahab Wahhab Kareem[1,2]
[1]Department of Information System Engineering, Polytechnic University Erbil, Iraq
[2]Department of Computer Technical Engineering, Al-Qalam University College, Kirkuk 36001, Iraq

ABSTRACT

Brain tumors, being the most severe and complex kind of cancer, necessitate specialized investigation for diagnosis, treatment, and care. Early recognition of brain tumors enhances patient care and reduces mortality rates. The application of deep learning in MRI diagnostics has transformed medicine. The study employs real and synthetic MRI data to evaluate novel deep-learning models to enhance brain tumor diagnosis. The ensemble model employed AlexNet, VGG16, and ResNet 18 on MR data from Rizgary Hospital in Erbil and Hiwa Hospital in Sulemani, as well as synthetic images produced by Deep Convolutional Generative Adversarial Networks. Modeling measurements encompassed accuracy, precision, recall, and F1 score. The architecture of ResNet18 and its capacity to incorporate residual connections for feature mapping enabled it to surpass all other models in classification accuracy, achieving 99%. Although AlexNet and VGG16 achieve accuracies of 98.16% and 98.83%, respectively, ResNet18 excels in differentiating between normal and unusual instances. DCGANs excel in generating synthetic images and enhancing image categorization and model precision. A study utilizing both real and synthetic images showed that synergistic virtual paradigms could enhance the accuracy of clinical instruments and facilitate deeper AI integration in medicine. Subsequent research will focus on optimizing model architecture and implementing data augmentation techniques to enhance classification accuracy. This Python study demonstrates that deep learning can enhance the diagnosis and treatment of brain tumors.

1.Introduction

Brain tumors arise from an abnormal increase of cells within the brain tissue and may be categorized as primary or secondary tumors. Primary tumors originate in the brain, while secondary tumors spread from different brain components. These tumors are, in addition, categorized as benign (non-cancerous) or malignant (cancerous). Malignant tumors, mainly at advanced levels, can be life-threatening. The recognition and categorization of brain tumors present great demanding situations due to variations in tumor size, form, and location among patients. Early and accurate prognosis is important for powerful treatment. Magnetic Resonance Imaging (MRI) is extensively used for brain tumor recognition as it provides high-resolution images of soft tissues and no longer involves dangerous radiation (Siva Raja & rani, 2020)(Haydar, 2022).

In the process of disease prediction, diagnosis, and treatment, the contributions of medical practitioners and researchers are of the utmost importance. On the other hand, one of the major challenges that these experts must contend with is a lack of datasets that are ample and diversified datasets (Johnson et al., 2021). The quantity of data that is utilized for training is a significant factor that determines the effectiveness of predictive models in the field of medical disease analysis (Candemir et al., 2021)(Abdullah et al., 2023).

Researchers have looked at methods of augmentation and the production of synthetic datasets as viable ways to expand and enhance the data that is currently accessible to meet the constraints that have been identified. (Khan et al., 2021), frequently conflate image enhancement with synthetic datasets. Nonetheless, a distinct distinction exists between augmentation and synthetic datasets. On the other hand, there is a distinct distinction between augmentation datasets and synthetic dataset samples. During the process of image augmentation, the training set is manipulated by modifying its geometric and color properties. These attributes include scaling, rotation, cutting, brightness, zooming in and out, and contrast (Alomar et al., 2023). One of the most significant drawbacks of using primary data or augmented data is that there is always the possibility of an accidental breach and an absence of preservation of the privacy of patients represented by the data. This is because the collection of data through Magnetic Resonance Imaging (MRI) may include images of the head, facial images, or comparable representations in a manner that enables the identities of research participants to be easily and accurately determined.(Anemone & Lalani, 2020)(A. I. Abdullah, 2020). On the contrary, synthetic data can be employed to get around this obstacle while also improving the efficiency of models in situations where the size of the data is insufficient to facilitate the training of models.

Synthetic datasets, on the other hand, are data that have been artificially manufactured and closely mirror the properties of source datasets. To establish supplementary or alternative data sources, particularly in scenarios with insufficient authentic data, synthetic datasets are manufactured artificially rather than derived from original data. Generative models, including generative adversarial networks (GANs) and Variational Autoencoders (VAEs), are commonly employed for synthetic data generation, alongside rule-based generators and simulation models(Wen et al., 2021). The application of GANs for producing synthetic medical research data represents a relatively unexplored methodology in current literature. Specifically in brain tumor prediction, GANs have not been extensively investigated for synthetic dataset generation, although some applications exist in medical image synthesis for brain tumor segmentation (Cirillo et al., 2021).

The potential of GANs for generating synthetic data to enhance brain cancer prediction models remains largely unexamined. This research aims to contribute significantly to illness prediction, particularly for brain tumors, which are increasing at an alarming rate globally due to stressful lifestyles and can significantly impact mortality rates if not detected early. Our work's primary contribution involves utilizing personally collected data while developing a Deep Convolutional Neural Network (DCNN) model based on CNN architectures for tumor recognition and

classification. We conduct a comprehensive performance comparison between our DCNN model and state-of-the-art models (ResNet18, VGG16, and AlexNet) when trained on both augmented and synthetic datasets. This comparative analysis evaluates the efficacy of these methodologies, determining which approach yields superior prediction accuracy while examining how synthetic datasets influence the predictive accuracy of illness models, particularly for brain cancers.

The main innovation of this manuscript involves the development of an ensemble deep learning architecture made from AlexNet, VGG16, and ResNet18, as well as their subsequent evaluation for brain tumor detection from MRI images. This merged architectural system leverages two separate CNN structures to raise diagnostic accuracy by exploiting their advantages. The research brings forward four primary achievements that include:

1-The manuscript brings together three pre-trained CNN frameworks (AlexNet and VGG16, and ResNet18) through weighted voting and majority rule methodology to optimize diagnostic identification results.
2-The merged network achieves enhanced diagnostic accuracy and reliability through model combination, which surpasses the performance of single network systems.
3-Turns out Transfer Learning makes the system learn efficiently from small medical image collections, whereas it minimizes both training time and computational requirements.
4-The ensemble framework provides early, precise tumor classification as part of clinical decision support that enables better quality medical decisions and treatment planning.
This paper follows this structure: Section I explores background information and motivation, with the study goals of brain tumor classification through MRI, along with deep learning. The second part of this paper illustrates a review of recent research regarding CNNs used for brain tumor recognition. The proposed ensemble framework, which incorporates AlexNet, VGG16, and ResNet18, forms the core of Section III (Methodology). Data collection, together with preprocessing operations, is expressed in this section as well. Experimental Setup and Results delivers descriptions of training procedures while presenting assessment parameters together with model-to-dataset performance assessments. Future research needs should be summarized in Section V (Conclusion), together with critical research findings.

2.Related work

The primary objective of this paper is to analyze and understand techniques for brain tumor categorization and recognition. This study aims to examine the most prevalent methods for recognizing brain cancer that are globally available, as well as to assess the efficacy of CAD systems in this context. The concept of GANs was initially introduced in (Mahdizadehaghdam et al., 2019). Backpropagation was the method that the researchers utilized to train their multilayer perceptron models for generators and discriminating factors. As a consequence of several improvements that have enhanced the quality of the images that are formed and broadened the variety of applications that can be used with them, GANs have gained a lot of popularity over the years. This popularity has gained a lot of momentum over the years. A particular architectural design that is referred to as the Deep Convolutional Generative Adversarial Network (DCGAN), as stated by(Radford et al., 2015), the goal is to reduce the disparity between the Convolutional Neural Networks (CNNs) that are used for supervised learning and those that are used for unsupervised learning. In (Onakpojeruo et al., 2024) version for classifying brain tumors, uses synthetic datasets generated through a Conditional Deep Convolutional Generative Adversarial Network (DCGAN) and traditional augmented datasets. The problem addressed is the scarcity of scientific datasets and privacy issues, with a look at innovatively leveraging GAN-generated artificial information for sickness classification duties. Using the Cancer Imaging Archive and KiTS19 datasets, the model was trained and tested on 40,000 preprocessed images, achieving 99% accuracy, precision, take into account, and F1 ratings for each dataset

kind. The C-DCNN outperformed modern-day models like VGG16, InceptionV3, and ResNet50, showcasing its robustness in correct diagnosis. This technique not only complements classification overall performance but also addresses information privacy concerns, making it a widespread contribution to clinical research and medical packages.(Li et al., 2020) introduces a unique combination of Deep Convolutional Generative Adversarial Networks (DCGAN) and AlexNet, for distinguishing pseudo progression (PsPD) from true tumor progression (TTP) in glioblastoma multiforme (GBM) the usage of MRI facts. The trouble addressed is the undertaking of differentiating PsPD and TTP, which exhibit similar visible characteristics in MRI, complicating medical remedy selections. The DC-AL GAN model leverages the opposed nature of GANs to extract high-level discriminative functions, with AlexNet as the discriminator.

A feature fusion technique is applied to mix high- and occasional-layer features, improving type performance. The version is evaluated on a dataset of 84 GBM patients, attaining a classification accuracy of 92%, outperforming different models, including DCGAN, ResNet, DenseNet, and VGG. The effects show the capacity of the DC-AL GAN for robust, automatic classification of PsP and TTP, addressing overfitting challenges and improving diagnostic accuracy in clinical settings(Sille et al., 2023). Makes a specialty of using Generative Adversarial Networks (GANs) for brain tumor segmentation. The problem addressed is the correct and automatic segmentation of brain tumors, which is important for analysis and treatment planning, especially for gliomas and glioblastomas. The look at leverages MRI images, particularly the use of facts from the BRATS 2020 database and other multimodal MRI benchmarks. The methodology involves using GAN-based total processes, including DCGAN and WGAN, to make the image resolution higher and improve segmentation accuracy.

The key contribution lies in showcasing GAN's capability to generate sensible pathological images and address the records augmentation demanding situations in clinical imaging. The outcomes highlight that GAN-based strategies achieved aggressive and promising results in segmenting brain tumors, with potential implications for enhancing future MRI-based diagnostic fashions.(Xu et al., 2024) addresses the venture of clinical image analysis with small, imbalanced datasets. The proposed answer introduces the Cross-Domain Attention-Guided GAN (CDA-GAN), a sophisticated CycleGAN model designed to generate clinically significant augmented data. The version consists of modern additives, such as the AMSE block for more desirable feature recalibration, a semi-supervised spatial interest module for unique location concentration, and spectral normalization to ensure training stability.

Experiments have been carried out at the BraTS 2020 and TCIA datasets, demonstrating improvements over ultra-modern techniques in class (e.g., 50% better accuracy and a pair of.05% higher F1 on BraTS) and segmentation responsibilities (e.g., 2.50% better Dice rating and 96.14% improvement in HD95 on TCIA). The contribution lies in successfully addressing inter-elegance differences and segmentation-demanding situations whilst proving the potential of go-domain statistics augmentation for clinical image tasks. A study on data augmentation strategies for brain tumor segmentation emphasized the advantages of GAN-based image augmentation and synthesis for brain tumors by (Nalepa et al., 2019). The researchers of (Safdar et al., 2020). While researchers have employed various strategies to enhance brain tumor classification using advanced models such as ResNet-50 and VGG-16, a significant gap persists in the literature. Despite the considerable accomplishments demonstrated in current studies, there remains an absence of thorough comparative analysis between synthetic and augmented dataset methodologies, specifically for medical disease prediction, particularly in the context of brain cancer. Although numerous investigations have examined the implementation of synthetic and augmented data approaches individually, they consistently fail to address the fundamental question regarding which methodology proves more appropriate and efficacious for medical

disease prediction. This critical comparison is essential for establishing optimal protocols in medical image analysis and could significantly impact diagnostic accuracy and treatment planning in clinical settings. Authors of (Iglesias et al., 2023). During the classification stage, the training sets are improved by the good quality and diversification offered by generative adversarial networks (GANs). It requires a generator to produce datasets that are as genuine as possible and a discriminator to distinguish between them. In the MRI image-based brain tumor classification problem, GANs create realistic MRI scans to overcome challenges like a limited and unbalanced dataset. The generator generates a fake image while the discriminator assesses whether the image formed is synthetic or real. Such an approach guarantees the progression of differences and improved realism in synthetic images. Thus, to increase classifier accuracy, the synthetic images produced within this classification framework can be incorporated into the training dataset. (Alrashedy et al., 2022) Previous research contrasted synthetic data with real data for blood glucose prediction; however, their work neither compared ML models with state-of-the-art approaches nor aligned with our current research objectives. A significant gap exists in the literature regarding studies that explicitly contrast synthetic and augmented image datasets generated by GANs for medical disease prediction. To our knowledge, this specific comparison remains unexplored in existing research. While some studies, such as(Mukherkjee et al., 2022)(Mustafa et al., 2024), have utilized GANs to augment data size for classification tasks using conventional ML models, they have not distinctly differentiated between synthetic generation and augmentation techniques, perpetuating the misconception that these approaches are equivalent. Our study addresses this critical gap, providing the medical research community with much-anticipated insights. We developed a novel CNN architecture specifically for brain tumor classification and systematically compared its performance against established models, including ResNet18, AlexNet, and VGG16, when trained on both augmented and purely synthetic datasets. The findings from this research enhance disease prognosis prediction accuracy and create new opportunities for medical research by establishing effective protocols for synthetic data utilization.The research evaluates modern developments in brain tumor discovery together with categorization and segmentation through Generative Adversarial Networks (GANs). At the beginning of their development, GANs were employed to synthesize medical images while handling data limitations and privacy challenges. High classification precision levels result from Conditional DCGANs along with DC-AL GANs, while surpassing the performance of VGG16 and ResNet50 as standard models. The performance of brain tumor segmentation has seen improvement with GAN-based approaches through their generation of detailed pathological images. The current literature shows limited research on the direct evaluation between artificial and augmented medical datasets in disease prediction tasks. The present research develops a new CNN model combined with a systematic analysis of dataset results to boost clinical research diagnostic precision and data augmentation implementation.

3.Materials and Methods

This section describes the procedures for data collection and analysis that were employed to accomplish the goals of the research, as well as the experimental design that is illustrated in Figure 1. This paper provides a comprehensive summary of all the models, processes, and techniques that were utilized in this research. Python, a programming language, was employed in Anaconda using a Spyder environment for training, testing, optimizing, and evaluating the model.

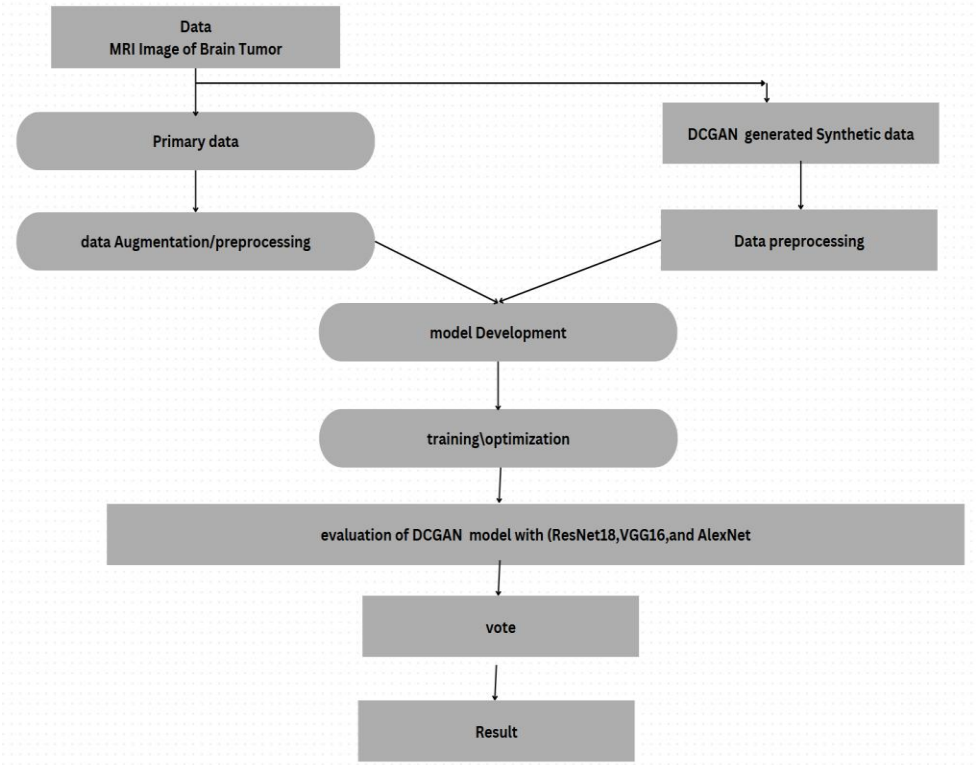

Figure 1 Study flow and experimental design

3.1Dataset

Brain MRI Images have been used to capture the brain tumor. As can be seen in Figure 2, the private dataset includes magnetic resonance imaging (MRI) in the Digital Imaging and Communications in Medicine (DICOM) format. Three months of data gathering were necessary to collect the dataset, which was obtained from a database maintained by Rizgary and Hiwa Hospital. Moreover, the classification process required an additional two to three months of development. Additionally, the database contains images that are both normal and abnormal.

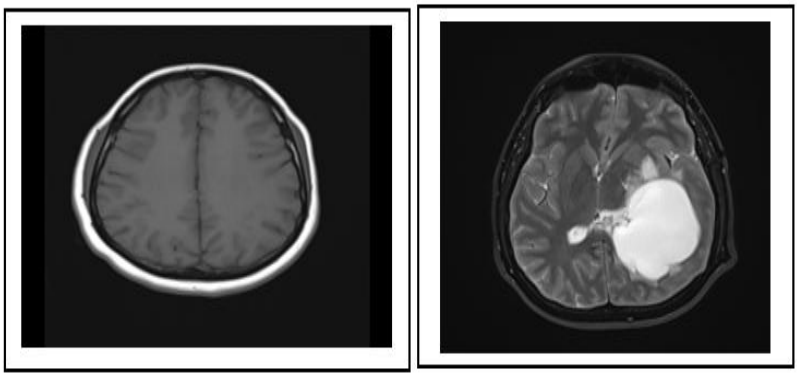

Figure 2 Example of an MRI

Magnetic resonance imaging (MRI) has a resolution of 512 by 512 pixels, and it contains a total of thousands of samples. A total of 200 patients' images are included in the dataset, with 15 images taken for each unique patient. Among these, one hundred cases were deemed to be abnormal, and another hundred cases were placed in the normal category. There were 38 male patients and 62 female patients in the dataset of normal cases, however, there were 67

male patients and 33 female patients in the abnormal instances, which indicates that males are infected with brain cancer. The hospitals in Erbil and Slemani provided the resources necessary to collect images of patients with brain cancer who ranged in age from 19 to 98. In addition, we used DCGAN to expand our data. We changed both the normal and abnormal from 1500 to 3000, each shown in Table 1.

Table 1: Dataset Detail

Brain tumor type	Real data	Synthetic data (using DCGAN)	Total	Training/testing data	Label
Normal	1500	1500	3000	80/20	0
Abnormal	1500	1500	3000	80/20	1

3.2. Image Preprocessing

Increasing the number of significant characteristics and fine details was accomplished through the elimination of superfluous variations using image pre-processing (Mustapha et al., 2022) . Images that had been preprocessed appropriately improved the segmentation and classification tasks (Ozsahin et al., 2023). This was because all algorithms were prone to noise. The size of the pixel region that is sought can be used to categorize the many techniques that are used for pre-processing images. These techniques employ the sub-images that surround the pixels to lessen the amount of noise and distortion in the image and improve its overall quality. Poor image quality, external factors, and a limited user interface can all cause MRI images to become distorted, which can result in a loss of visual information and processing problems. (Mustapha et al., 2022). Nevertheless, these biases can be avoided through the use of proper preprocessing methods. For the given analysis, the addition of contrast was done to draw more attention to specific areas of interest in the dataset. The primary collection of brain cancer data was composed of MRI images in DICOM format, which poses serious problems for CNN frameworks due to its proprietary structure, lack of supporting tools, and possible conflicts with other software. These DICOM images are much easier to handle in JPEG (Joint Photographic Experts Group) format, as it is considerably more compatible with CNN frameworks and reduces overall file sizes. Therefore, all DICOM images were converted to JPEG format. After this conversion, each image was processed further by resizing and normalizing the image, preparing it for analysis with neural networks, and then saving it in JPEG format. The augmentation techniques added diverse methods to generate more training data that expanded the available effective dataset.

1. The process of image rotation occurred across a spectrum of angles from -30 to +30 degrees.
2. The application of both horizontal and vertical flips generated mirrored duplicates of the original image files.
3. A brightness adjustment frame ranged between ±20 to enhance the images.

These augmentation techniques effectively multiplied the training data, creating variations of existing images with different orientations, perspectives, and lighting conditions. This expanded dataset helped prevent overfitting and improved the models' ability to recognize brain tumors under various imaging conditions and orientations without requiring additional patient scans

3.3 Model Architecture

Three cutting-edge deep learning models that are used for classifying brain cancer using magnetic resonance imaging (MRI) have been implemented and analyzed. ReseNet18, VGG16, and AlexNet were chosen for their robust architectural strengths in data categorization. With the identification of an acceptable methodology for identifying brain cancers using magnetic resonance imaging (MRI) and the utilization of deep learning algorithms for efficient and reliable diagnosis, the approach was examined in greater depth.

3.3.1 Generative Adversarial Networks (GAN)

Generative Adversarial Networks (GANs) are

a framework for training a deep learning model to replicate the distribution of training data, enabling the generation of new data from that same distribution. They consist of two separate models: a generator and a discriminator. The generator's function is to produce 'synthetic' images that resemble the training images. The discriminator's role is to evaluate an image and determine if it is a genuine training image or a counterfeit image produced by the generator (Jenkins & Roy, 2024). Throughout the training process, the generator persistently endeavors to surpass the discriminator by producing increasingly sophisticated fakes, while the discriminator strives to enhance its recognition capabilities to accurately distinguish between real and counterfeit images(Park et al., 2021). The equilibrium of this game occurs when the generator produces flawless fakes indistinguishable from the training data, while the discriminator consistently guesses with 50% confidence whether the generator's output is real or fabricated.

Let x Data that represents an image.$D(x)$ is the discriminator network that outputs the scalar probability indicating whether x Originated from the training data instead of the generator. The input to $D(x)$ is an image with a Channels Height Width(CHW) size of 3x64x64. Intuitively, $D(x)$ should be HIGH when x originates from the training data and LOW when x It is produced by the generator. $D(x)$ may also be regarded as a conventional binary classifier. In the generator's nomenclature, let z Represent a latent space vector drawn from a typical normal distribution. G (z) denotes the generating function that transforms the latent vector z Into data space. The objective of G It is to approximate the distribution from which the training data originates (p_{data}) to facilitate the generation of synthetic samples from the estimated distribution (p_{g}).$D(G\ (z))$)is the scalar probability that the output of the generator G It is a genuine image. In(*Unsupervised Representation Learning with Deep Convolutional Generative Adversarial Networks*, n.d.), D and G Engage in a minimax game where D aims to maximize the likelihood of accurately classifying real and fake instances ($log\ \ D(x)$), while G seeks to reduce the probability that D will classify its outputs as false ($log\ (1-D(G\ (z)))$)The loss function for the GAN is delineated as follows:

$$\text{Min}_G\ \text{Max}_D V\ (D,G)=E_{x\sim p_{data(x)}}[\log D(x)]+E_{z\sim pz(z)}[\log(1-D(G(z))] \quad (1)$$

Where:

$p_{dat}(x)$ is the distribution of real data.

$p_z(z)$ is the prior distribution of the input noise variable z.

$G(z)$ is the generator mapping from noise to data space.

$D(x)$ outputs the probability that x came from real data rather than the generator.

The theoretical solution to this minimax game occurs when $p_g = p_{data}$, and the discriminator randomly determines whether the inputs are authentic or counterfeit. Nonetheless, the convergence theory of GANs remains a subject of active investigation, and in practice, models do not consistently reach this state.(Mahdizadehaghdam et al., 2019).

3.3.1.1Deep Convolutional Generative Network (DCGAN)

A Deep Convolutional Generative Adversarial Network (DCGAN) is a direct extension of the GAN described earlier, except that it makes explicit use of convolutional and convolutional-transpose layers in the discriminator and generator, respectively. Stride convolution layers, batch norm layers, and LeakyReLU activations are the components that make up the discriminator. Input is a 3x64x64 image, and output is a scalar probability that the input is from the real data distribution. The input is the image, and the output is the probability. Convolutional-transpose layers, batch norm layers, and ReLU activations are the components that make up the generator. In this study, DCGAN was employed. DCGAN is a specific type of GAN designed to generate high-quality synthetic images(Onakpojeruo et al., 2024)(Goodfellow et al., 2020). DCGANs employ CNNs as both the discriminator and generator. DCGANs have been extensively utilized and adapted for many imaging production tasks, including object recognition, handwriting recognition, facial age progression, and realistic faces and scenes. They have made a substantial contribution to the field of generative models(Behara et al.,

2023)(Alrashedy et al., 2022). The Generator network is expected to convert the noise vectors to realistic image attributions. They use architectures based on a deep convolution layer, which transforms the five-input feature maps at different rates while up-sampling until images of the size 64×64 pixels and three-color channels are produced. The network starts with an input of a latent noise vector of dimension 100 and applies several transposed convolution layers($G(z;\theta_g)$: $R^{100}\rightarrow R^{H\times W\times C}$), also known as deconvolution layers. There are a total of three blocks in the architecture for up-sampling operations. The first block converts the input noise, as passed through the latent dim, into 512 feature maps. Subsequently, the network continues with three more blocks that progressively reduce the number of feature maps while increasing the spatial dimensions from 512:256 to 128:64 channels. Each of those blocks is made of a transposed convolution layer with a batch normalization layer and a ReLU function for introducing non-linearity. The last layer of the Generator also employs a transposed convolution to generate the final output image with 3 channels – RGB; the final activation function used is Tanh to scale the generated values to the range of [-1,1]. This architecture allows the Generator, through the training phase, to learn the mapping of random noise to realistic image distributions($D(x;\theta_d)$: $R^{H\times W\times C}\rightarrow[0,1]$). Therefore, the discriminator adversarial training.

network is adversarial, and it is designed to learn the images that have been generated and the real ones. The system is designed following a convolutional neural network structure, which gradually reduces the spatial size of the input image whilst adding extra feature channels. Figure 3: DCGAN diagram of the Generator and discriminator. The network, first of all, consists of the initial convolution block, which takes the input image with three channels and produces 64 Feature Maps. This first block has a missing feature from batch normalization to have the discriminator learn directly from input statistics. The architecture then continues with three additional blocks that progressively increase the number of feature maps while reducing spatial dimensions: from 64 to 128 channels, from 128 to 256 channels, and from 256 to 512 channels. Every block of the discriminator includes a convolutional layer, LeakyReLU function with a negative slope of 0.2, and batch normalization, but for the first block. The final layer performs a convolution that will squash feature maps down to a single channel. Then a sigmoidal function is applied, which spits out the Discriminator's evaluation of the input image: is it real, or is it fake? They both employ a kernel size of 4 in their architectures and employ suitable stride and padding parameters to obtain the specific spatial transformations. All the above architectural choices allow the networks to learn the distribution of the target image dataset using

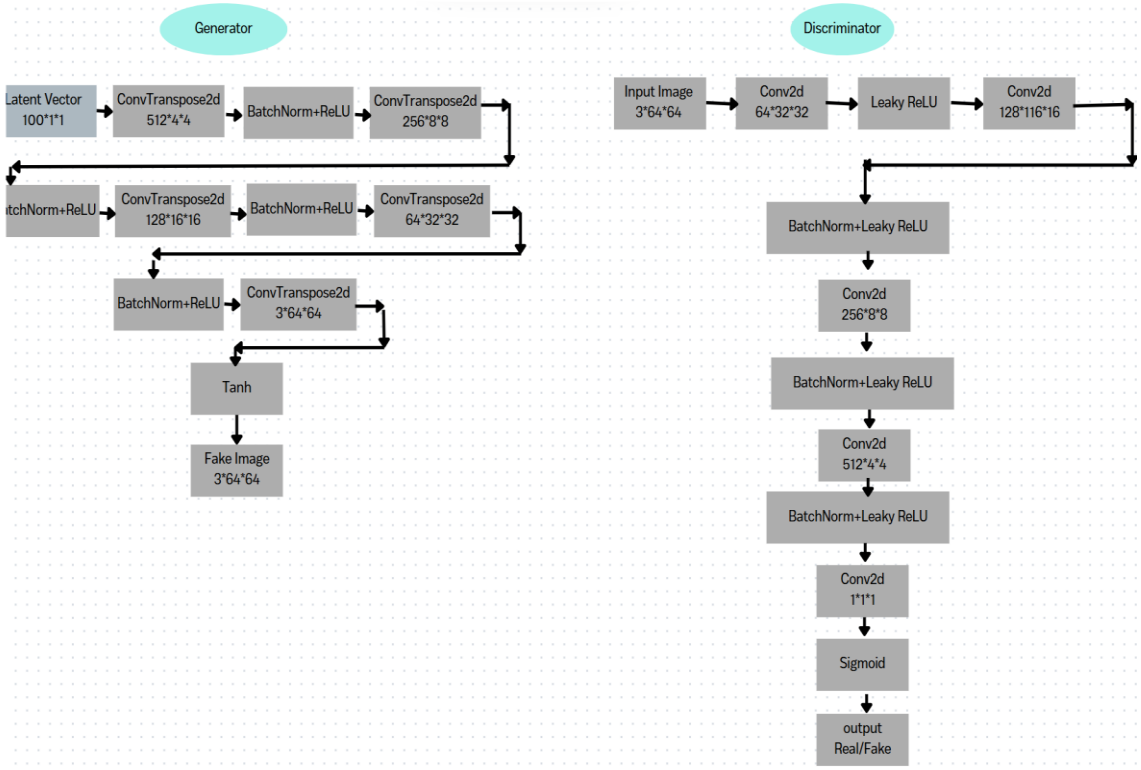

Figure 3: DCGAN diagram of the Generator and discriminator.

Training Dynamics

The training process involves alternating between updating the discriminator and the generator:

Update Discriminator:

- Real images: Maximize log$D(x)$
- Fake images: Maximize log(1−$D(G(z))$)
- Combined objective: max$_D$ $E_{x\sim p_{data}(x)}$[log$D(x)$]+$E_{z\sim pz(z)}$[log(1−$D(G(z))$] (2)

Update Generator:

- In practice, instead of minimizing log(1−$D(G(z))$)We maximize log$D(G(z))$ to provide stronger gradients early in training
- Objective: max$_G$ $E_{z\sim pz(z)}$ [log$D(G(z))$]

The gradient updates for the discriminator parameters are

$$\nabla_{\theta d}\frac{1}{m}\sum_{i=0}^{m}[logD(x)^{(i)} + \log\left(1 - D(G(z)^{(i)})\right)] \quad (3)$$

The gradient updates for the generator parameters are:

$$\nabla_{\theta d}\frac{1}{m}\sum_{i=0}^{m}[logD\left(x\right)^{(i)}) \quad (4)$$

- Where m is the mini-batch size.

This adversarial process continues until the generator learns to produce images that the discriminator cannot distinguish from real ones.(Peng et al., 2025). Figure 4 shows the architecture of DCGAN.

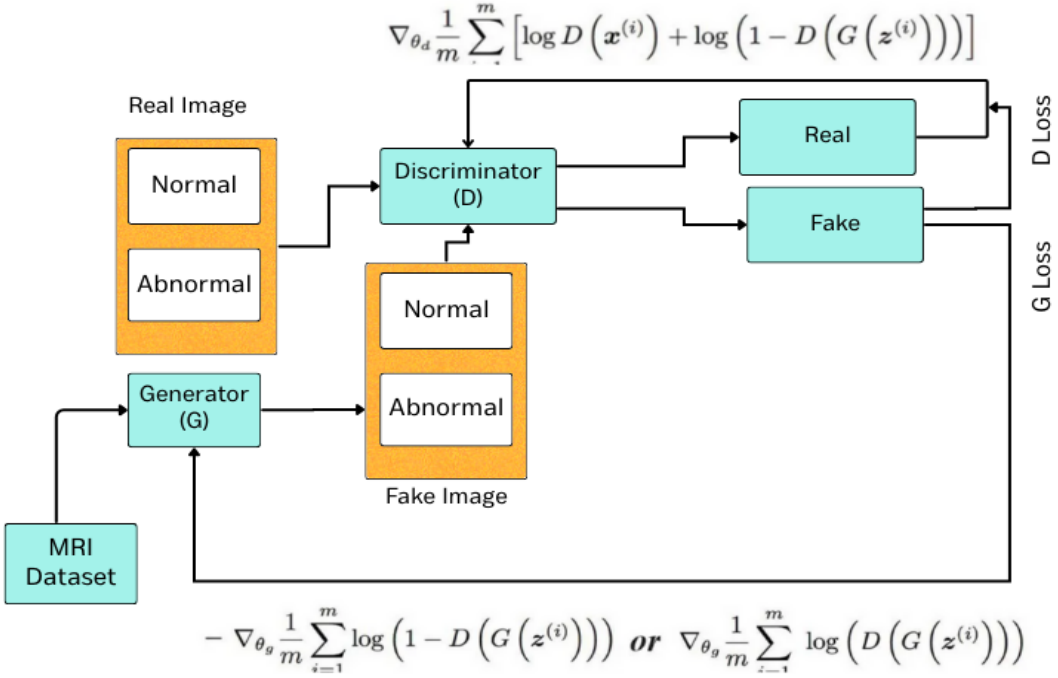

Figure 4:DCGAN architecture

3.3.2 ResNet

A deep resident network (ResNet) model that is founded on deep architectures and demonstrates high levels of accuracy and high levels of accuracy. ResNet was developed by a number of the surviving stacked units, and it has been constructed with a variety of layer numbers, including 18, 34, 50, 101, 152, and 1202. ResNet 18 is a decent compromise between performance and depth, although the number of operations can vary depending on the architectures that are used(El-Feshawy et al., 2023). ResNet architecture, and especially ResNet-18, is used for medical imaging tasks, including the diagnosis of Alzheimer's disease, because of the ability of the proposed framework to effectively learn multi-level patterns. Residual learning is the idea of creating layers of a network such that the layers learn residual functions rather than direct functions, making the optimization process easier since optimizations are done on differences between input and output. This approach minimizes the degradation problem that is common with deeper networks in which accuracy flattens or even declines as depth rises. Figure 5 shows the architecture diagram of ResNet18, how the layers are laid own, and how they are connected. As a result, there is the encouragement of very deep networks and, at the same time, the enhancement of accuracy, which makes ResNet well-suited for classifying complex patterns in medical images like MRI scans. (ZainEldin et al., 2023). It is because of its dependability and versatility that ResNet has become a model that is utilized more frequently to transfer learning between a number of different activities. Due to its capacity to train extremely deep neural networks, ResNet has become a point of reference in the field of deep learning. It has been demonstrated that when deep learning is performed well within trained models, it produces superior outcomes. (Ramtekkar et al., 2023). An overview of the ResNet model is provided, as shown in Table 2.

Table 2 Outline of the ResNet18 model

Name of layer	Size of output	ResNet 18
Convolution1	112*112*64	7*7,64, stride 2
Convolution3	28*28*128	1283*3 convolutions
Convolution4	14*14*256	2563*3 convolutions
Convolution5	7*7*512	5123*3 convolutions
Average pool	1*1*512	7*7 Average pool
Fully connected	2	512*2 fully connected
Soft max	2	----

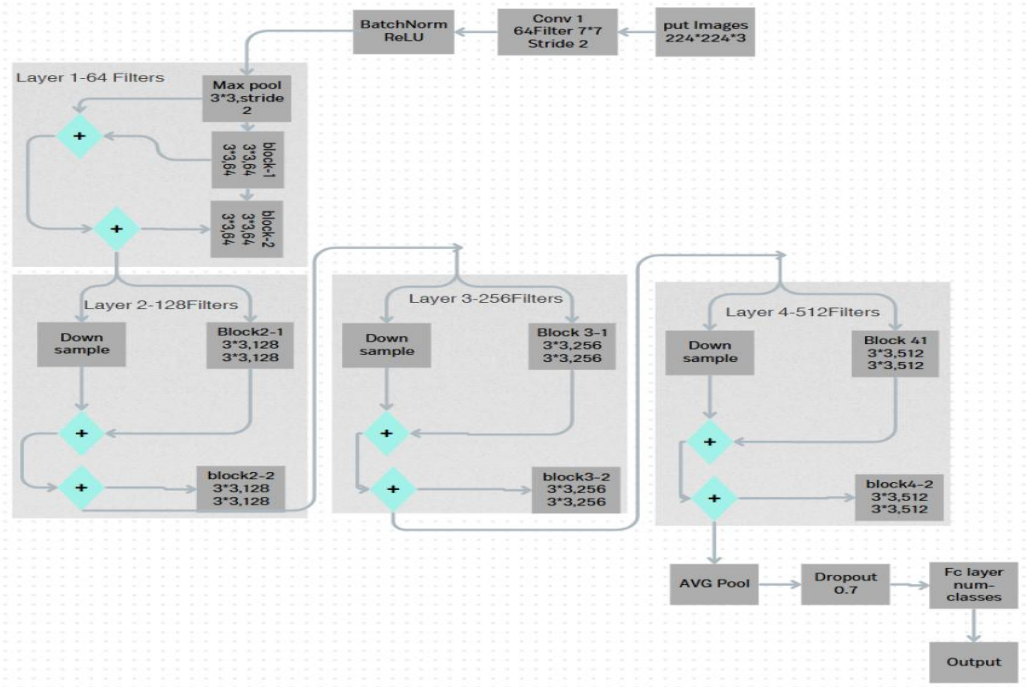

Figure 5: ResNet architecture diagram

3.3.3VGG16

VGG Transfer Learning VGG is a neural network trained on the ImageNet dataset for the classification of natural images(Al-Mukhtar et al., 2023). The VGG16 architecture, introduced by Simonyan and Zisserman, has a fixed input size of 224 × 224. The images are processed through a series of convolutional layers utilizing small receptive filters of 3 × 3. Additionally, 1 × 1 convolution filters are employed to perform a linear transformation of input channels, followed by a non-linear activation. To maintain spatial resolution post-convolution, a padding of 1 pixel is utilized for 3 × 3 convolutional layers; spatial pooling is performed using 5 max-pooling layers. Max pooling is executed using a 2×2-pixel window with a stride of 2. A series of convolutional layers is followed by three fully connected (FC) layers, where the first two FC levels have 4096 channels each, and the third FC layer comprises 1000 channels, corresponding to each class. The ultimate layer of this architecture is the SoftMax layer.(Ramzan et al., 2020). Figure 6 shows the architecture diagram of VGG16.

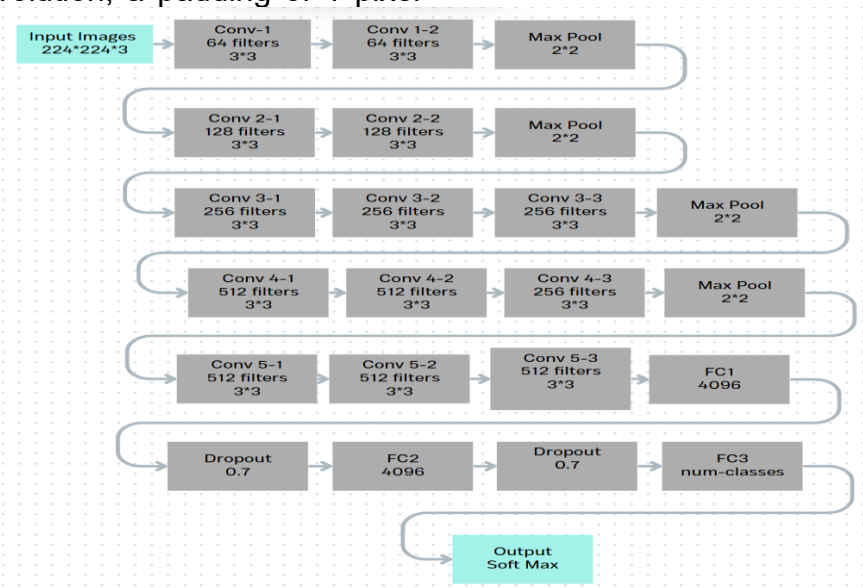

Figure 6: VGG16 architecture diagram

3.3.4 AlexNet

The AlexNet is a conventional convolutional neural network that made a major image recognition advancement when it garnered the 2012 ImageNet challenge. The network design takes an input of 227X227X3 RGB images and comprises the following units: five convolutional layers, three fully connected layers. The first Layer type is Convolution, and the number of filters is 96, the size is 11*11, and stride is 4, the Second Layer type is Convolution and the filters is 256 of size 5*5, the Layer type is Convolution and the number of filters is 3*3 containing 384, 384 and 256 respectively. The constraints imposed by the need to limit processing time are satisfied through the inclusion of three max pooling layers of kernel 3 × 3 and stride 2 in the sequel of the network after the first, second, and fifth convolution layer. After that, the network goes through to three completely connected layers, the two initial ones containing 4096 neurons each, and the last one representing the number of the target categories. Activation functions deployed throughout the network is ReLU, while the regularization technique between FC layers is dropout with a probability of 0.7. It finishes at a softmax layer for classification, and it is most beneficial for large-scale image classification.(Putzu et al., 2020). Figure 6 shows the architecture diagram of AlexNet.

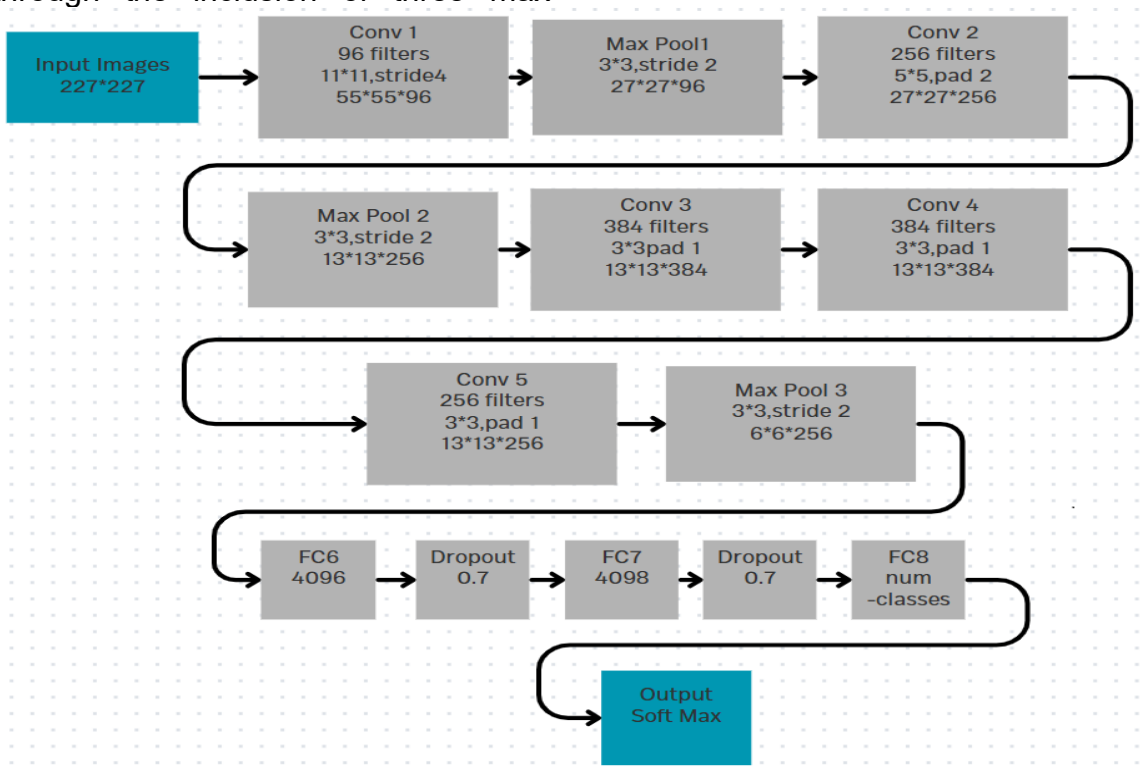

Figure 7: AlexNet architecture diagram

3.4 Optimization and Hyperparameter Tuning

In particular, noted that with a project such as designing and implementing a deep convolutional neural network-based DCGAN, hyperparameter tuning was required as the model's performance and training efficiency were affected greatly with poorly optimized parameters. It is well known that the parameters set by the researchers will influence performance aspects related to capacity, regularization, and convergence speed [30]. In the case of the DCGAN intern, we made several hyperparameter changes to improve learning rates (0.1 – 0.3), beta 1 of 0.5 for the exponential decay rate within Adam's optimizer, batch sizes between 8 and 128, fixed noise dimension of 100, and epochs ranging from 50 up to thousands dependent on the model's complexity. We considered appropriate complexity for a set architecture for the generator and discriminator for the specific application. Regarding the classification task

done through well-known models such as ResNet18, VGG16, and AlexNet, they distinctively chose not to change their original hyperparameters, valuing the benefits achieved through transfer learning, as alteration would have fundamentally changed the construction and operation of the models. For the novel CNN model developed, we utilized a grid search optimization approach to test multiple combinations of parameters in order to determine the best-performing set. The key hyperparameters explored included batch sizes from 10 to 100, epochs ranging from 30 to 100, five optimizers (SGD, AdamW, Adam, Adamax, and Nadam), and various learning rates (0.0001, 0.001, 0.01, 0.1, 0.2, and 0.003). After thorough evaluation, our grid-search determined the optimal configuration consisted of 32 batches, 50 epochs, Adam optimizer, and a 0.0001 learning rate, maximizing model efficacy while preventing issues such as slow convergence or overfitting..

3.5 Evaluating Methods

This substantiates the study's validity. The suggested model evaluation, detailed in equations (5) to (8), encompasses four metrics: accuracy, precision, Recall, and F1-Score (FS). In this context, TP represents true positives, TN denotes true negatives, FP indicates false positives, and FN suggests false negatives.

- **Accuracy**: Accuracy refers to the ratio of the true patterns to the summation of entire patterns. It can be expressed as

$$\text{Accuracy} = \frac{True\ Positive + True\ \text{Negative}}{\text{True Positives + False Positives+True Negative+False Negative}}\ 100 \quad (5)$$

- **Precision**: The percentage of accurately projected positive observations to the total projected positives.

$$\text{Precision} = \frac{True\ Positive}{\text{True Positives + False Positives}} \quad (6)$$

Greater precision shows less false positives

- **Recall** (or sensitivity): The percentage of accurately projected positive observations to all actual positives.

$$\text{Recall} = \frac{True\ Positive}{\text{True Positives + False Negative}}. \quad (7)$$

Greater recall shows less false negative

- **F1-Score**: The harmonic means of precision and recall.

$$\text{F1}_{\text{score}} = \frac{2\times\text{Precision}\times\text{Recall}}{\text{Precision +Recall}} \quad (8)$$

A high F1 score shows that the model balances precision and recall in between [-1,1]. Our learning method repeatedly alternates between developing the discriminator network and the generator network during the training steps. In each epoch, the generator creates false images using random numbers then the discriminator checks these images against the actual ones. Our training records losses alongside images it generates at every single epoch step. Our system shows real and fake images next to each other with loss curves for both networks as training progresses. The completed generator becomes our future model

4.Preparing and assessing experiments

In this experiment, a huge dataset of images consisting of 3000 images was obtained from 200 patients, of whom 1500 were benign and 1500 were malignant. All of the data was gathered within a period of 3 months at Erbil Rzgray Hospital and Sulaymaniyah Hewa Hospital. DCGAN implementation runs on Pytorch to generate images. We transform the dataset through four steps that include resizing images, cropping them in the center, transforming to tensors, and normalizing values

while we track training results through multiple plots that show the improvement of both models over time. The hyperparameter tuning is shown in Table (3).

Table 3: DCGAN hyperparameters

Parameter	Value	Description
latent dim	100	Dimension of the noise vector input
image size	64	Size of input/output images (64x64)
Num channels	3	Number of color channels (RGB)
batch size	16	Number of images per training batch
learning rate	0.0002	Learning rate for Adam optimizer
Epochs	1500	Total number of training epochs
optimizer betas	(0.5,0.999)	Beta parameters for Adam optimizer
normalization range	[-1,1]	Input image normalization range

And below procedure of DCGAN model that have been used in the paper is added:

DCGAN implementation:
• Setup
- Set device (GPU/CPU)
- Initialize hyperparameters (latent_dim=100, image_size=64)
- Load and transform dataset
• Networks
- Generator: noise → fake images
- Discriminator: images → real/fake probability
• Training Loop
- For each epoch:
* Generate fake images from noise
* Train discriminator (real + fake images)
* Train generator
* Save losses and sample images
• Output
- Save model
- Plot results and losses

which were also utilized, in order to guarantee the efficiency of the training and testing stages. We have prepared our model according to the results shown in table (4).

Table 4: Hyperparameters of transfer learning models for image classification

Quantifying performance and evaluation	Assessing measurement outcomes
Batch size	32
Optimizer	Adam
Number of epochs	50
Learning rate	0.0001
Evaluation criterion	cross-entropy loss function
Training	confusion matrices

The evaluated models, ResNet18 exhibited superior performance, achieving the lowest testing loss of 0. 0235.at epoch 30 and a testing accuracy of 99.33.00% Among the evaluated models, AlexNet exhibited the lowest testing loss of 0.1026 at epoch 32 but experienced the most fluctuation in testing accuracy. It ultimately achieved a testing accuracy of 98.17%. VGG16 showed promising results, with accomplishing training of accuracy 98.83% and loss of 0.0426 at the epoch 39. An ensemble of three models combines their predictions to enhance accuracy and robustness. This can be executed through strategies like voting (majority or weighted), where the final output is primarily based on the consensus or confidence of each model, for brain tumor classification, an ensemble of ResNet18, VGG16, and AlexNet should use majority or weighted voting to supply extra reliable predictions.

5.Experimental results and comparison

5.1Results & Discussion

The results gotten from the deep learning models shows that convolutional neural networks (CNNs) are useful in classifying brain tumors using MRI images. ResNet18 is the model with the highest accuracy, which means it performs best out of all models at feature extraction from medical imaging data. This is due to the architecture's residual connections which decrease the vanishing gradient problem and allow lower performance walls for deeper

structures. VGG16 and AlexNet also show decent performance but do lag in results because their simpler architecture does not perform as well. These results mean deeper networks can improve diagnosed performance in medical imaging when trained right, regulated, and some sort of learning enabled. Further evaluation on larger, diverse datasets is still needed to test if the accuracy is reliable. Alongside model comparison, the fact that certain MRIs were real and others were not aided in the training's robustness. Created synthetic data works to relieve classification issues posed by being an underrepresented class or having a few samples in comparison with a class—all to improve the actual dataset. The overall enhancement allowed limited overfitting by boosting generalization, especially for deeper models like ResNet18, leading to fewer duplicate discrepancies. Focus on cautious realism should be a focus while model training using synthetic data.

for this work, Python programming language was used in the Spyder Notebook environment for training and testing models using both real datasets and the synthetic dataset that was developed. The pre-processed data, which totaled 6000, and consisted of three thousand real data and three thousand synthetic data, were divided into two sets: a training set consisting of 80%, and a test set consisting of 20% for both synthetic and real data. Subsequently, these datasets have been integrated into the novel CNN model. This strategy ensured that the model was robust and generalized well to data that had not been seen before, illustrating the benefits of combining both synthetic data and real data simultaneously in the training process. The training of the model lasted for 50 epochs. Furthermore, we used DCGAN to expand locally created dataset . We had 1500 normal and 1500 abnormal brain tumor images. We put both datasets separately in DCGAN, which then gave us 3000 normal and 3000 abnormal synthetic data. Figure 8 shows an example of the real and fake images. Figure 9 shows the generator and discriminator loss during training.

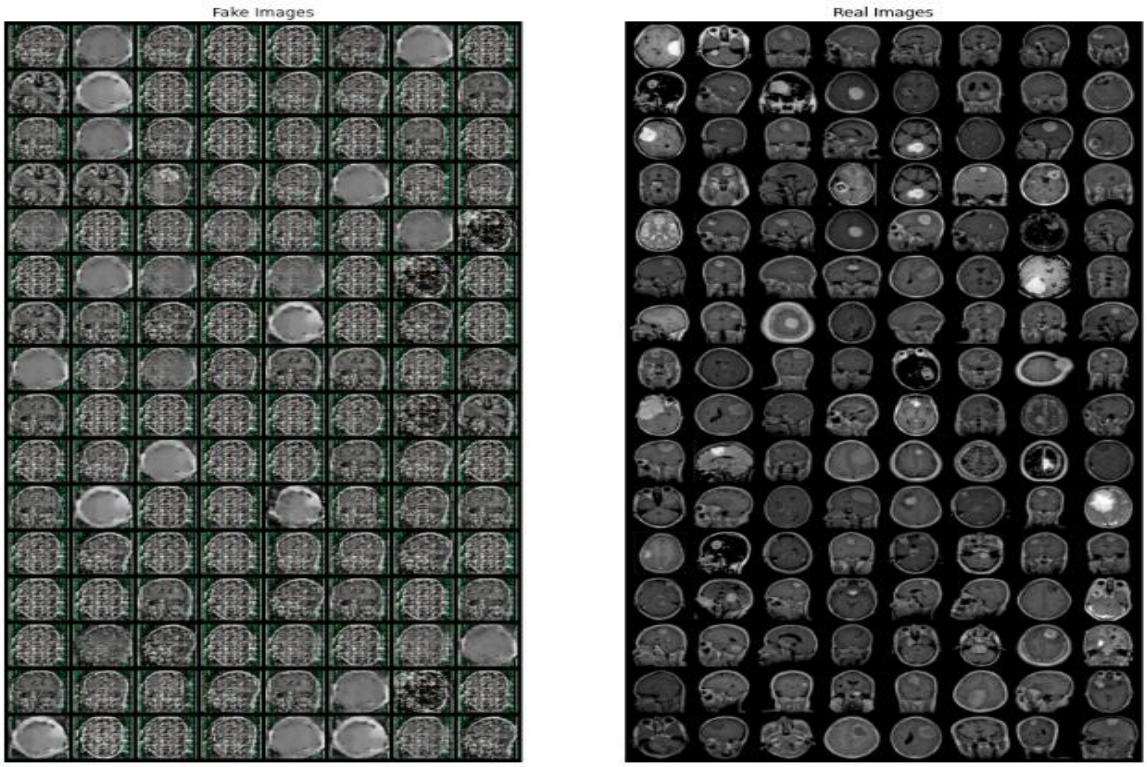

Figure 8: Real and Fake images

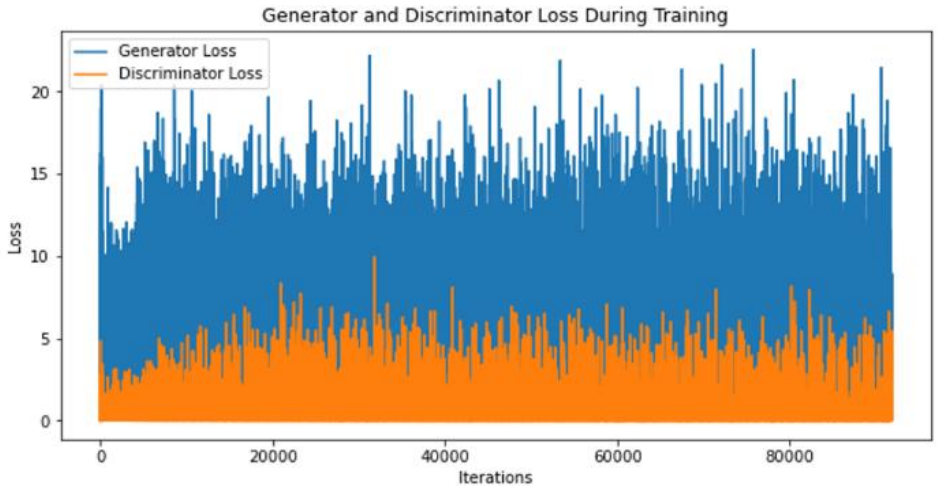

Figure 9: generator and discriminator loss

Research used ResNet18 VGG16 plus AlexNet versions of CNN architecture for the dataset. we tested the models exclusively with actual data and synthetic the results are shown in table (5).

Table 5: Testing All Models

model		type	precision	recall	f1-score	Accuracy
ResNet18	**Testing**	normal	0.99	0.99	0.99	99
		abnormal	0.99	0.99	0.99	
VGG16	**Testing**	normal	0.98	1	0.99	98.83
		abnormal	1	0.98	0.99	
AlexNet	**Testing**	normal	0.97	0.99	0.98	98.16
		abnormal	0.99	0.97	0.98	

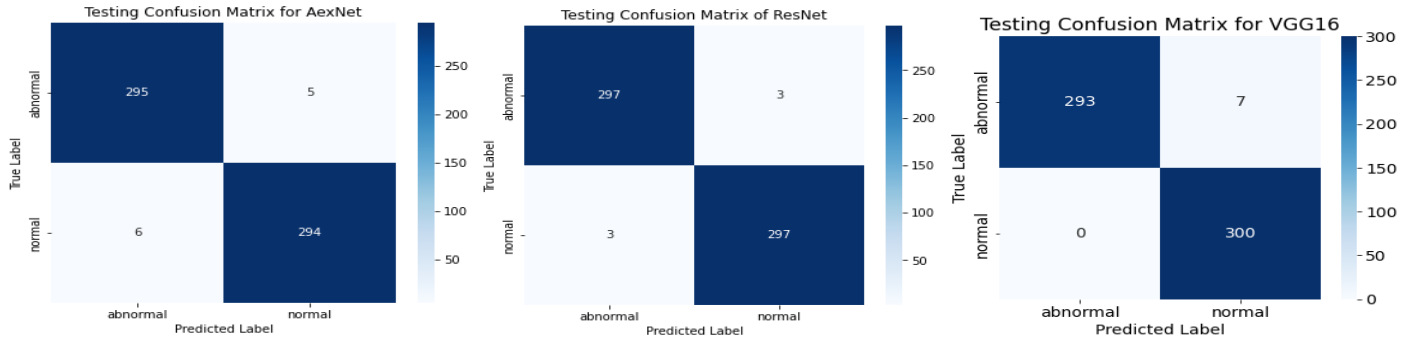

Figure (10 a b c) shows the confusion matrix of all three models

Among the models that were assessed, ResNet18 performed the best, attaining a testing loss of 0.0410 at epoch 50 and a testing accuracy of 99.24%. AlexNet had the lowest testing loss of 0.0804 at epoch 13 of the models that were assessed, but it also had the highest variability in testing accuracy. In the end, it reached a testing accuracy of 98.75%. VGG16 produced encouraging results, achieving a training accuracy of 98.92% and a loss of 0.0873 at epoch 48. The results of the three models from each epoch are described in the figures below. Moreover, Figures (11,12,13) show the accuracy and loss of all three models.

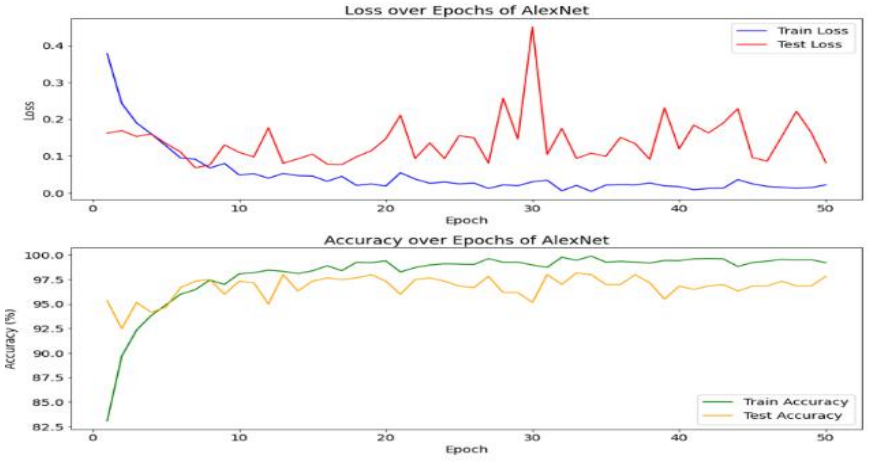

Figure 11: Training and testing loss and Accuracy of AlexNet

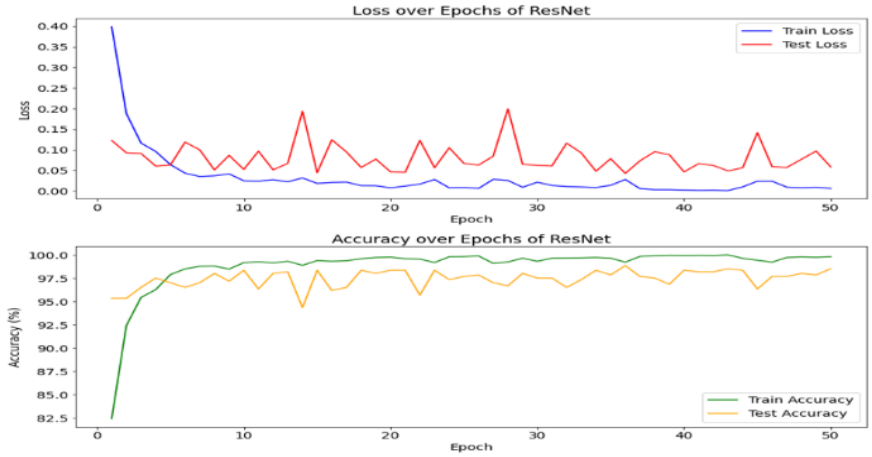

Figure 12: Training and testing loss and Accuracy of ResNet

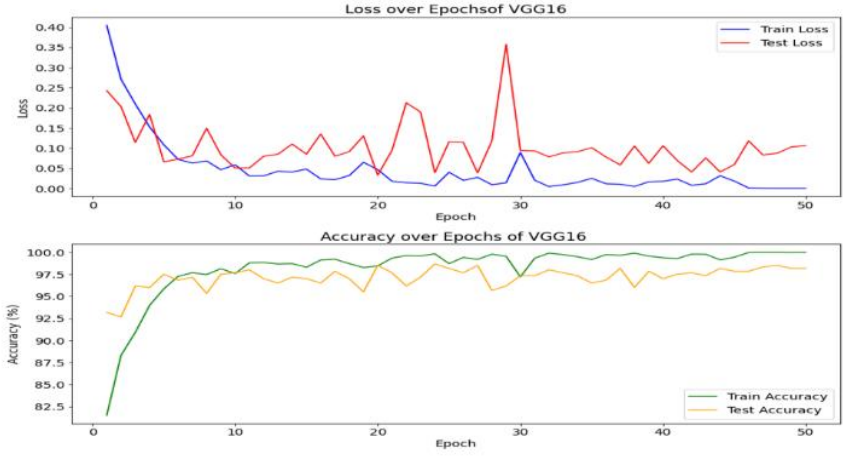

Figure 13: Training and testing loss and Accuracy of VGG16

Figure 14 illustrates the ROC curves for all three models. ResNet is exceptionally proficient in differentiating between the two classes, exhibiting minimal false positives and a high rate of true positives across various thresholds. An AUC of (1) demonstrates high model performance. VGG16 also had a proficient ROC curve with a result of (1), and lastly, AlexNet had an ROC curve result of (1).

The three models worked together to aggregate their predictions in order to improve accuracy and strength. This can be accomplished using

procedures such as voting (majority or weighted), in which the final result is mostly determined by the consensus or confidence of each model. When classifying brain tumors, an ensemble of ResNet18, VGG16, and AlexNet should use majority or weighted voting to provide more credible predictions. In addition, we obtained the ensemble predictions of all the models combined. The majority voting was 98.68%, and the weighting voting was also 98.68%. Finally, we also found the ROC curves. Figure (15) shows the architecture of the Ensemble model and an AUC of (1) and plot accuracies for the models over the epochs as shown in figures (16,17).

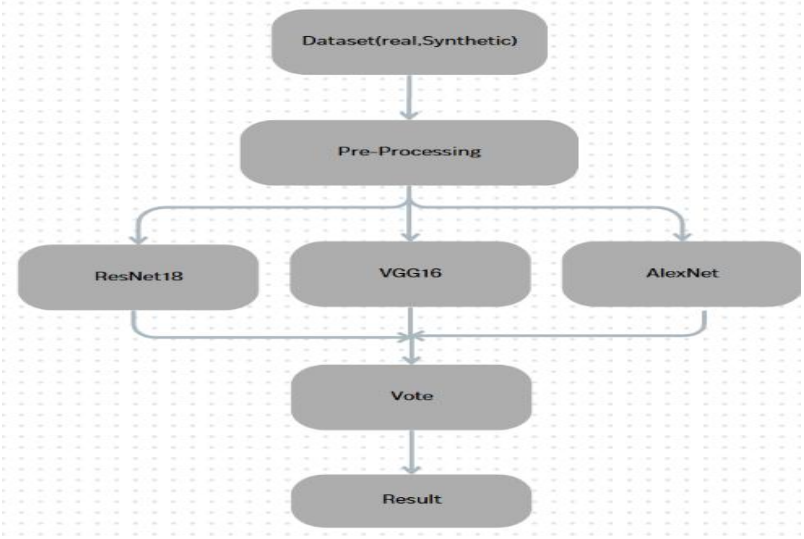

Figure 10: Ensemble of AlexNet, ResNetv18, VGG16

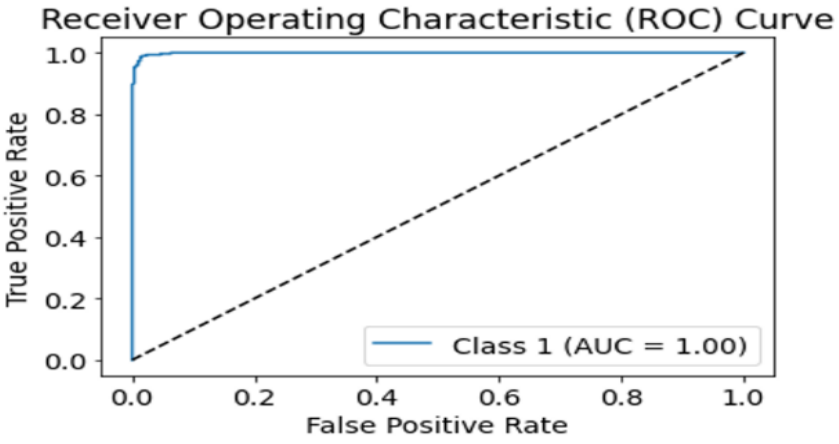

Figure 15: ROC Curve

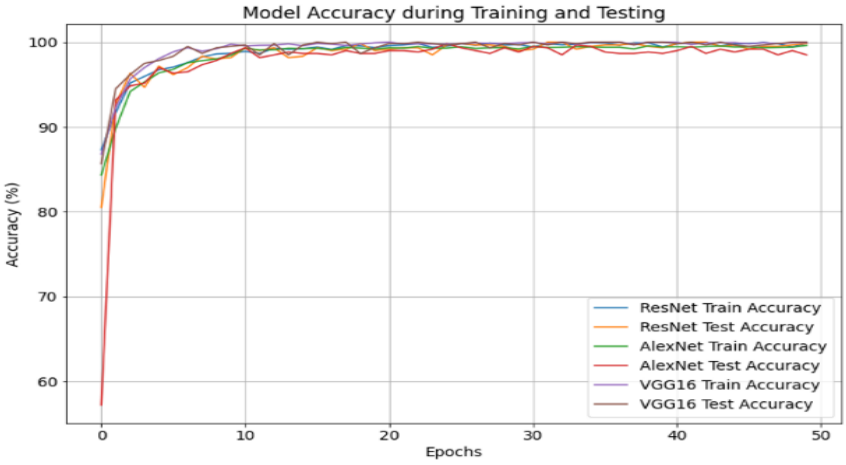

Figure16: Ensemble accuracy of AlexNet, ResNetv18, VGG16.

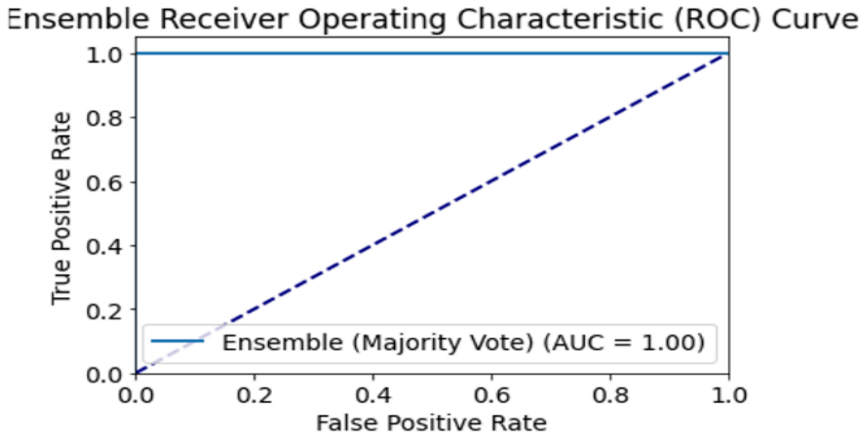

Figure 11: ROC curve Ensemble of AlexNet, ResNetv18, VGG16

5.2Comparison

Fo analyzing the research model which has been developed is generalized and it can classify blur or noise added images and keeps its accuracy, A comparison has been done between three models (ResNet18, VGG16, AlexNet) without having DCGAN data and one with the GAN data both using the collected dataset as you can see the details in table 6. The investigation demonstrated ResNet18 delivered the finest overall operational outcomes by obtaining 99% precision and recall as well as f1-score across real normal data and real abnormal data and real data augmented with synthetic entries. VGG16 and AlexNet also showed strong results, with precision, recall, and f1-scores generally in the 96-99% range. The models performed better on the real with synthetic data compared to the real data alone, indicating the benefits of data augmentation. The abnormal data cases tended to have slightly lower precision but higher recall, suggesting the models are better able to identify abnormal samples. The ensemble performance, which combines the predictions of multiple models, reached 98-99% across the different data types and model architectures. The deep learning models demonstrated excellent performance on this classification task, with ResNet18 emerging as the top performer. The implementation of augmented data significantly improved system accuracy.

Table 6: Model Performance Comparison

Type of data	Models	Type	Precision (%)	Recall (%)	f1score (%)	AUC (%)	Accuracy (%)	Ensemble (%)
Real data	ResNet18	Normal	99	98	99	1	98.66	98.33
		Abnormal	98	99	99			
	VGG16	Normal	96	99	98	1	97.83	
		Abnormal	99	96	98			
	AlexNet	Normal	99	98	98	1	97.66	
		Abnormal	98	99	98			
Real+synthetic data	ResNet18	Normal	99	99	99	1	99	98.67
		Abnormal	99	99	99			
	VGG16	Normal	98	1	99		98.83	
		Abnormal	1	98	99			
	AlexNet	Normal	98	98	98	1	98.16	
		Abnormal	98	98	98			

results show that DCGAN consistently improves CNN performance by a small amount across different models. The CNN accuracy scores rise consistently when DCGAN integration patterns appear across all ResNet, VGG16, and AlexNet testing shown in figure 17.

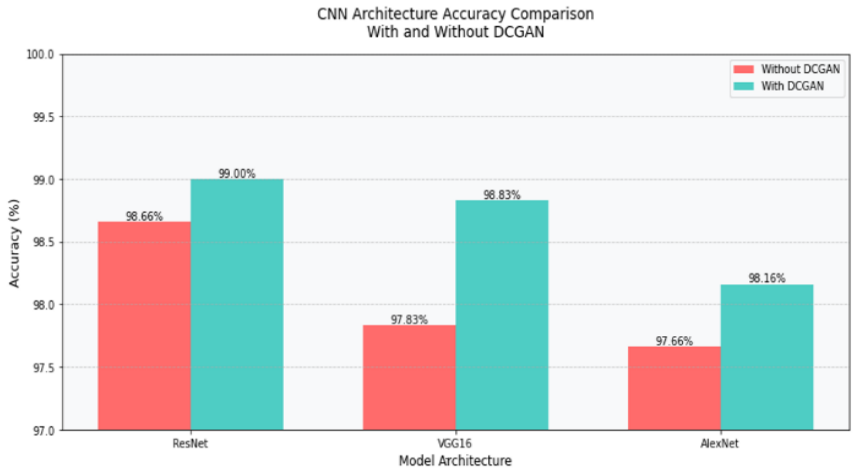

Figure 12: CNN Architecture Accuracy Comparison with and Without DCGAN

5.3Brain Tumor Image Dataset with Grayscale Normalization and Zoom (3096 images)

The dataset was brought from Kaggle, it consists of 3096 brain images which used to be 3264 images that has been developed and upgraded, which contains normal and abnormal. As shown in table (7) I applied my methods on the Kaggle dataset first I used DCGAN and made the synthetic data then I used my three models (VGG16, ResNet, and AlexNet) on both the real and synthetic data, comparing the methods: The DCGAN method making use of ResNet, VGG16, and AlexNet performed superior performance with accuracies of 99.98%, 99.35%, and 99.03%, extensively outperforming different methods. The next first-rate performer was the multi-model method the usage of Xception, DenseNet-201, and EfficientNet-B3 at 97.74%, observed by

means of the CNN ensemble at 97.12%. AlexNet with VGG and ResNet achieved 96.94%, the VGG16/ResNet18/Dense Net aggregate reached 95%, and the ResNet50/VGG16 pairing showed the lowest accuracy at 92.6%. the method used in my model had the highest accuracy and the methos used.

Table 7: Performance Comparison of Brain Tumor Image Dataset with Grayscale Normalization and Zoom

Method	Accuracy (%)
CNN, ResNet50, InceptionV3, InceptionResNetV2, Xception,MobileNetV2, and EfficientNetB0(Gómez-Guzmán et al., 2023)	97.12
VGG16, ResNet18, and DenseNet(Nigjeh et al., 2024)	95
Multi model of (Xception, DenseNet-201, and EfficientNet-B3)(Santoso et al., 2024)	97.74
ResNet50,VGG16(F. Abdullah et al., 2024)	92.6
AlexNet,VGG,ResNet(Wang et al., 2024)	96.94
our model (DCGAN apply (ResNet, VGG16, and AlexNet))	99.98, 99.35,99.03

6.Conclusion

This groundbreaking study showed the profound potential of deep learning for brain tumor classification by developing new techniques for fusion of real and synthetic MRI image datasets. Integration of high-quality synthetic data generated by DCGAN technology into a CNN ensemble comprising ResNet18, VGG16, and AlexNet yielded astounding diagnostic accuracy of 99% for brain tumor identification. The research offered a novel solution to fundamental challenges in medical imaging diagnosis by providing patient-validated MRI scans that synthesized clinical imaging with zeroes data, data range limitations, and privacy issues, along with data scarcity, dataset scope, and patient data confidentiality. By collecting MRI images from patients at Rizgary Hospital in Erbil and Hiwa Hospital in Sulemani, then with aid of DCGAN augmenting the dataset from 1500 to 3000 images including normal and abnormal categories, a comprehensive dataset was created. The study is the first to show the reliable accuracy improvement achieved through the inclusion of synthetic data across multiple CNNs, thus achieving a new frontier for AI in Medicine. The use of ResNet18 as a voting block for VGG16 and AlexNet in the ensemble increased the diagnostic accuracy for complex cases, demonstrating the power of cooperation among deep learning models. Combining ResNet18 with VGG16 and AlexNet using weighted voting demonstrated greater reliability in diagnosing complex conditions showcasing the power of deep learning collaboration. In regard to tumor cases, precise diagnostic methodologies in parallel with advanced brain imaging techniques greatly aid in patient management by heightening survival rates and improving treatment strategies, placing focus on the recognition of malignant tumors at the initial growth stage. Along with further exceptional strides, the AI-driven framework alongside the medical imaging systems tailored for healthcare services underscored the evolution of deep learning allied with generative adversarial networks and ensemble modeling techniques, unlocking opportunities in medical image classification and underscoring the capacity of AI in redefining diagnostics toward systemic shifts not only in medical care, but also in clinical decision support systems.

7.Reference

Abdullah, A. I. (2020). Brain Cancer Medical Diagnostic System Using Grey Scale Features and Support Vector Machine. *Zanco Journal of Pure and Applied Sciences*, *32*(3). https://doi.org/10.21271/zjpas.32.3.5

Abdullah, F., Jamil, A., Alazawi, E. M., & Hameed, A. A. (2024). Exploring Deep Learning-based Approaches for Brain Tumor Diagnosis from MRI Images. *2024 IEEE 3rd International Conference on Computing and Machine Intelligence, ICMI 2024 - Proceedings*. https://doi.org/10.1109/ICMI60790.2024.10585851.

Abdullah, R. M., Masseh, H. D. I., Salihi, A. & Faraj, B. M. (2023). Unleashing the Power of OpenAI in Shaping the Future of Cancer Research. *BioMed Target Journal*, 1, 2-11. https://doi.org/10.59786/bmtj.112

Al-Mukhtar, F. H., Ismael, D. S., Yousif, R. Z., Haji, S. O., & Mohammed, B. (2023). Thyroid Nodule Image Joint Segmentation and Classification Based on Deep Learning. *Zanco Journal of Pure and Applied Sciences*, 35(5), 60–71. https://doi.org/10.21271/ZJPAS.35.5.6

Alomar, K., Aysel, H. I., & Cai, X. (2023). Data Augmentation in Classification and Segmentation: A Survey and New Strategies. *Journal of Imaging*, *9*(2).

https://doi.org/10.3390/jimaging9020046
Alrashedy, H. H. N., Almansour, A. F., Ibrahim, D. M., & Hammoudeh, M. A. A. (2022). BrainGAN: Brain MRI Image Generation and Classification Framework Using GAN Architectures and CNN Models. *Sensors*, *22*(11). https://doi.org/10.3390/s22114297
Anemone, S., & Lalani, T. (2020). Patient Friendly Summary of the ACR Appropriateness Criteria: Acute Mental Status Change, Delirium, and New Onset Psychosis. *Journal of the American College of Radiology*, *17*(9), e50. https://doi.org/10.1016/j.jacr.2020.04.011
Behara, K., Bhero, E., & Agee, J. T. (2023). Skin Lesion Synthesis and Classification Using an Improved DCGAN Classifier. *Diagnostics*, *13*(16). https://doi.org/10.3390/diagnostics13162635
Candemir, S., Nguyen, X. V., Folio, L. R., & Prevedello, L. M. (2021). Training strategies for radiology deep learning models in data-limited scenarios. *Radiology: Artificial Intelligence*, *3*(6). https://doi.org/10.1148/ryai.2021210014
Cirillo, M. D., Abramian, D., & Eklund, A. (2021). Vox2Vox: 3D-GAN for Brain Tumour Segmentation. *Lecture Notes in Computer Science (Including Subseries Lecture Notes in Artificial Intelligence and Lecture Notes in Bioinformatics)*, *12658 LNCS*, 274–284. https://doi.org/10.1007/978-3-030-72084-1_25
El-Feshawy, S. A., Saad, W., Shokair, M., & Dessouky, M. (2023). IoT framework for brain tumor detection based on optimized modified ResNet 18 (OMRES). *Journal of Supercomputing*, *79*(1), 1081–1110. https://doi.org/10.1007/s11227-022-04678-y
Gómez-Guzmán, M. A., Jiménez-Beristaín, L., García-Guerrero, E. E., López-Bonilla, O. R., Tamayo-Perez, U. J., Esqueda-Elizondo, J. J., Palomino-Vizcaino, K., & Inzunza-González, E. (2023). Classifying Brain Tumors on Magnetic Resonance Imaging by Using Convolutional Neural Networks. *Electronics (Switzerland)*, *12*(4), 1–22. https://doi.org/10.3390/electronics12040955
Goodfellow, I., Pouget-Abadie, J., Mirza, M., Xu, B., Warde-Farley, D., Ozair, S., Courville, A., & Bengio, Y. (2020). Generative adversarial networks. *Communications of the ACM*, *63*(11), 139–144. https://doi.org/10.1145/3422622
Haydar, C. A. M. A. (2022). Comprehensive Study for Breast Cancer Using Deep Learning and Traditional Machine Learning. *ZANCO JOURNAL OF PURE AND APPLIED SCIENCES*, *34*(2). https://doi.org/10.21271/ZJPAS.34.2.3)
Iglesias, G., Talavera, E., González-Prieto, Á., Mozo, A., & Gómez-Canaval, S. (2023). Data Augmentation techniques in time series domain: a survey and taxonomy. *Neural Computing and Applications*, *35*(14), 10123–10145. https://doi.org/10.1007/s00521-023-08459-3
Jenkins, J., & Roy, K. (2024). Exploring deep convolutional generative adversarial networks (DCGAN) in biometric systems : a survey study. *Discover Artificial Intelligence*. https://doi.org/10.1007/s44163-024-00138-z
Johnson, K. B., Wei, W. Q., Weeraratne, D., Frisse, M. E., Misulis, K., Rhee, K., Zhao, J., & Snowdon, J. L. (2021). Precision Medicine, AI, and the Future of Personalized Health Care. *Clinical and Translational Science*, *14*(1), 86–93. https://doi.org/10.1111/cts.12884
Khan, A. R., Khan, S., Harouni, M., Abbasi, R., Iqbal, S., & Mehmood, Z. (2021). Brain tumor segmentation using K-means clustering and deep learning with synthetic data augmentation for classification. *Microscopy Research and Technique*, *84*(7), 1389–1399. https://doi.org/10.1002/jemt.23694
Li, M., Tang, H., Chan, M. D., Zhou, X., & Qian, X. (2020). DC-AL GAN: Pseudoprogression and true tumor progression of glioblastoma multiform image classification based on DCGAN and AlexNet. *Medical Physics*, *47*(3), 1139–1150. https://doi.org/10.1002/mp.14003
Mahdizadehaghdam, S., Panahi, A., & Krim, H. (2019). Sparse generative adversarial network. *Proceedings - 2019 International Conference on Computer Vision Workshop, ICCVW 2019*, 3063–3071. https://doi.org/10.1109/ICCVW.2019.00369
Mahmood, D. A. & Aminfar, S. A. (2024). Efficient Machine Learning and Deep Learning Techniques for Detection of Breast Cancer Tumor. *BioMed Target Journal*, 2, 1 - 13. https://doi.org/10.59786/bmtj.211
Mukherkjee, D., Saha, P., Kaplun, D., Sinitca, A., & Sarkar, R. (2022). Brain tumor image generation using an aggregation of GAN models with style transfer. *Scientific Reports*, *12*(1), 1–16. https://doi.org/10.1038/s41598-022-12646-y
Mustafa, O. S., Askar, S. K., Karim, S. W., & Hussein, B. K. (2024). Emotion Recognition in Kurdish Speech from the Sorani Dialect Corpus. *Zanco Journal of Pure and Applied Sciences*, *36*(5), 104–112. https://doi.org/10.21271/ZJPAS.36.5.10
Mustapha, M. T., Ozsahin, D. U., Ozsahin, I., & Uzun, B. (2022). Breast Cancer Screening Based on Supervised Learning and Multi-Criteria Decision-Making. *Diagnostics*, *12*(6), 1–17. https://doi.org/10.3390/diagnostics12061326
Nalepa, J., Marcinkiewicz, M., & Kawulok, M. (2019). Data Augmentation for Brain-Tumor Segmentation: A Review. *Frontiers in Computational Neuroscience*, *13*(December), 1–18. https://doi.org/10.3389/fncom.2019.00083
Nigjeh, M. K., Ajami, H., Mahmud, A., Hoque, S. U., & Umbaugh, S. E. (2024). *Comparative Analysis of Deep Learning Models for Brain Tumor Classification in MRI Images Using Enhanced Preprocessing Techniques*. *13137*, 1–5. https://doi.org/10.1117/12.3028318
Onakpojeruo, E. P., Mustapha, M. T., Ozsahin, D. U., & Ozsahin, I. (2024). A Comparative Analysis of the Novel Conditional Deep Convolutional Neural Network Model, Using Conditional Deep Convolutional Generative Adversarial Network-Generated Synthetic

and Augmented Brain Tumor Datasets for Image Classification. *Brain Sciences*, *14*(6). https://doi.org/10.3390/brainsci14060559

Ozsahin, D. U., Onakpojeruo, E. P., Uzun, B., & Mustapha, M. T. (2023). *Mathematical Assessment of Machinarning Models Usede Le*. 1–12. https://doi.org/10.3390/%0Adiagnostics13040618

Park, S., Ko, J., Huh, J., & Kim, J. (2021). *Review on Generative Adversarial Networks : Focusing on Computer Vision and Its Applications*. 1–40.

Peng, K., Huang, D., & Chen, Y. (2025). Retinal OCT image classification based on MGR‐GAN. *Medical & Biological Engineering & Computing*, *0123456789*. https://doi.org/10.1007/s11517-025-03286-1

Putzu, L., Piras, L., & Giacinto, G. (2020). Convolutional neural networks for relevance feedback in content based image retrieval: A Content based image retrieval system that exploits convolutional neural networks both for feature extraction and for relevance feedback. *Multimedia Tools and Applications*, *79*(37–38), 26995–27021. https://doi.org/10.1007/s11042-020-09292-9

Radford, A., Metz, L., & Chintala, S. (2015). Unsupervised Representation Learning with Deep Convolutional Generative Adversarial Networks. *4th International Conference on Learning Representations, ICLR 2016 - Conference Track Proceedings*, 1–16. https://doi.org/10.48550/arXiv.1511.06434

Ramtekkar, P. K., Pandey, A., & Pawar, M. K. (2023). Accurate detection of brain tumor using optimized feature selection based on deep learning techniques. In *Multimedia Tools and Applications* (Vol. 82, Issue 29). Springer US. https://doi.org/10.1007/s11042-023-15239-7

Ramzan, F., Khan, M. U. G., Rehmat, A., Iqbal, S., Saba, T., Rehman, A., & Mehmood, Z. (2020). A Deep Learning Approach for Automated Diagnosis and Multi-Class Classification of Alzheimer's Disease Stages Using Resting-State fMRI and Residual Neural Networks. *Journal of Medical Systems*, *44*(2). https://doi.org/10.1007/s10916-019-1475-2

Safdar, M. F., Alkobaisi, S. S., & Zahra, F. T. (2020). A comparative analysis of data augmentation approaches for magnetic resonance imaging (MRI) scan images of brain tumor. *Acta Informatica Medica*, *28*(1), 29–36. https://doi.org/10.5455/AIM.2020.28.29-36

Santoso, I. B., Supriyono, & Utama, S. N. (2024). Multi-Model of Convolutional Neural Networks for Brain Tumor Classification in Magnetic Resonance Imaging Images. *International Journal of Intelligent Engineering and Systems*, *17*(5), 741–758. https://doi.org/10.22266/ijies2024.1031.56

Sille, R., Choudhury, T., Sharma, A., Chauhan, P., Tomar, R., & Sharma, D. (2023). A Novel Generative Adversarial Network-Based Approach for Automated Brain Tumour Segmentation. *Medicina (Lithuania)*, *59*(1). https://doi.org/10.3390/medicina59010119

Siva Raja, P. M., & rani, A. V. (2020). Brain tumor classification using a hybrid deep autoencoder with Bayesian fuzzy clustering-based segmentation approach. *Biocybernetics and Biomedical Engineering*, *40*(1), 440–453. https://doi.org/10.1016/j.bbe.2020.01.006

Unsupervised Representation Learning with Deep Convolutional Generative Adversarial Networks. (n.d.). https://doi.org/10.48550/arXiv.1511.06434

Wang, J., He, L., & Zhou, X. (2024). Optimizing Inception-V3 for Brain Tumor Classification Using Hybrid Precision Training and Cosine Annealing Learning Rate. *2024 7th International Conference on Advanced Algorithms and Control Engineering, ICAACE 2024*, 528–532. https://doi.org/10.1109/ICAACE61206.2024.10548577

Wen, Q., Sun, L., Yang, F., Song, X., Gao, J., Wang, X., & Xu, H. (2021). Time Series Data Augmentation for Deep Learning: A Survey. *IJCAI International Joint Conference on Artificial Intelligence*, 4653–4660. https://doi.org/10.24963/ijcai.2021/631

Xu, Z., Tang, J., Qi, C., Yao, D., Liu, C., Zhan, Y., & Lukasiewicz, T. (2024). Cross-domain attention-guided generative data augmentation for medical image analysis with limited data. *Computers in Biology and Medicine*, *168*(April 2023), 107744. https://doi.org/10.1016/j.compbiomed.2023.107744

ZainEldin, H., Gamel, S. A., El-Kenawy, E. S. M., Alharbi, A. H., Khafaga, D. S., Ibrahim, A., & Talaat, F. M. (2023). Brain Tumor Detection and Classification Using Deep Learning and Sine-Cosine Fitness Grey Wolf Optimization. *Bioengineering*, *10*(1), 1–19. https://doi.org/10.3390/bioengineering10010018.